Journal of Molecular Spectroscopy 378 (2021) 111455

Contents lists available at ScienceDirect

Journal of Molecular Spectroscopy

journal homepage: www.elsevier.com/locate/jms

High-resolution laser spectroscopy of the $\tilde{A}^1\Pi_u - \tilde{X}^1\Sigma_g^+$ transition of $^{13}C^{12}C^{12}C$ and $^{12}C^{13}C^{12}C$

Qiang Zhang [a], Jingwang Gu [a], Kirstin D. Doney [b], Harold Linnartz [b], Yang Chen [a], Dongfeng Zhao [a,*]

[a] Hefei National Laboratory for Physical Sciences at the Microscale, University of Science and Technology of China, 230026 Hefei, PR China
[b] Laboratory for Astrophysics, Leiden Observatory, Leiden University, PO Box 9513, NL2300 RA Leiden, the Netherlands

ARTICLE INFO

Article history:
Received 31 December 2020
In revised form 18 March 2021
Accepted 20 March 2021
Available online 5 April 2021

Keywords:
C_3
High-resolution spectroscopy
Laser-induced fluorescence
Isotopologue

ABSTRACT

We present a laser spectroscopic study of the $\tilde{A}^1\Pi_u - \tilde{X}^1\Sigma_g^+$ transition of ^{13}C mono-substituted C_3 in the 378–406 nm region. The $^{13}C^{12}C^{12}C$ and $^{12}C^{13}C^{12}C$ isotopologues are produced in a pulsed jet expansion, by DC discharging a gas mixture of ~0.3% C_2H_2/Ar (with ~1% ^{13}C natural abundance). By using laser induced fluorescence spectroscopy, thirteen vibronic bands belonging to the $\tilde{A}^1\Pi_u - \tilde{X}^1\Sigma_g^+$ electronic transition have been recorded for $^{13}C^{12}C^{12}C$ and $^{12}C^{13}C^{12}C$, eleven of which have not been reported before. The transitions cover the three fundamental vibrational modes (v_1, v_2^l, v_3). For all the vibronic bands, the full width at half maximum of spectral lines is found to be narrower than 0.023 cm^{-1}, allowing to determine the transition frequencies with an absolute accuracy of ~0.003 cm^{-1}. Moreover, rotational analyses of the high-resolution data have yielded accurate spectroscopic constants for the upper vibronic states studied here. The 100–000, 04^+0–000 and 12^-0–000 bands of $^{13}C^{12}C^{12}C$, and the 02^+0–000 and 04^-0–000 bands of $^{12}C^{13}C^{12}C$ are found to be less blended by spectral features of $^{12}C_3$, and thus may be used for astronomical searches of $^{13}C^{12}C^{12}C$ and $^{12}C^{13}C^{12}C$ in the space.

1. Introduction

The bare carbon chain molecule propadienediylidene, C_3, has received considerable attention because of its important astronomical role. This small molecule is a potential intermediate in the formation of longer carbon chains and carbonaceous circumstellar grains, and is considered a likely fragment upon photo- or electron-dissociation of larger molecules [1]. Furthermore, its widespread distribution in a variety of astronomical environments renders C_3 a good diagnostic probe for astrochemical research. As C_3 has a linear centro-symmetric structure, it is 'radio-silent', but, its electronic and vibrational transitions in the optical and infrared (IR) regions, respectively, provide spectroscopic alternatives for detecting and tracing this simple molecule in space.

Since the first identification of the 4050 Å band in cometary emission [2], C_3 has been detected in the comae of numerous comets as well as in the atmospheres of cool stars (see Refs. [3–5] and references therein). The presence of C_3 in the diffuse interstellar medium (ISM) was confirmed in direct absorption by Maier et al. [6] and subsequent observations in the sightlines of other stars were reported [7–10]. Recently, Schmidt et al. [11] reported detection of eight vibronic bands in the $\tilde{A}^1\Pi_u - \tilde{X}^1\Sigma_g^+$ transition of C_3, seven of which were identified for the first time, in a translucent cloud towards HD 169454. These assignments became only possible following new laboratory data obtained by the same authors.

In much higher density environments, C_3 has also been detected via its infrared signatures. In 1988, Hinkle et al. observed the v_3 anti-symmetric stretch vibration around 5 μm in the circumstellar envelope IRC + 10216 [12]. About one decade later, a low-resolution interstellar absorption feature in the far-IR region observed toward Sgr B2(M) was assigned to the C_3 v_2 bending vibration by Cernicharo et al. [13]. Soon after that, Giesen et al. discussed new laboratory data on the vibrational spectrum of C_3 in its low-frequency bending mode and re-visited the first identification of the v_2 R(2) line in absorption toward Sgr B2(M) [14]. Recently, high-resolution observations using the Herschel/HIFI instrument resulted in v_2 transitions originating in the warm envelopes of massive star-forming regions [15]. Later, a post warm-up model was proposed to explain the formation chemistry of C_3 in the star-forming cores associated with the DR21(OH) region, based on the observed far-IR spectra [16]. Besides the main isotopologue C_3, ^{13}C-isomers of C_3 have also been identified in the ISM recently. Giesen et al. [17] reported the first detection of $^{13}C^{12}C^{12}C$ and $^{12}C^{13}C^{12}C$ isotopologues towards Sgr B2(M) via their v_2 transition.

* Corresponding author.
E-mail address: dzhao@ustc.edu.cn (D. Zhao).

https://doi.org/10.1016/j.jms.2021.111455
0022-2852/

The $^{12}C/^{13}C$ abundance ratio in the C_3 molecules was derived as 20.5 ±4.2 and a gas excitation temperature of $44.4^{+4.7}_{-3.9}$ K was found.

The many observational studies prompted the need for additional high-resolution laboratory studies of C_3 that led to more accurate spectroscopic data. In return, laboratory data assisted further detections of C_3 in the ISM, providing new insights on the chemical processes taking place in different regions. So far, numerous laboratory studies have been reported on the main isotopologue, $^{12}C^{12}C^{12}C$, including the $\tilde{A}\ ^1\Pi_u - \tilde{X}^1\Sigma_g^+$ optical transition as well as the rovibrational IR spectra (see Refs. [3,14,18–39]). By contrast, less studies have been reported on the ^{13}C-substituted isotopologues. In 1951, Douglas et al. obtained the 4050 Å band heads for the six isotopologues ($^{12}C_3$, $^{13}C^{12}C^{12}C$, $^{12}C^{13}C^{12}C$, $^{13}C^{13}C^{12}C$, $^{13}C^{12}C^{13}C$, and $^{13}C_3$), and identified C_3 as the carrier of the 4050 Å band [21]. Soon after, this conclusion was further confirmed by Clusius *et al.* who analyzed the rotationally resolved spectrum of the same band for $^{13}C_3$ [40]. Recently, rotationally resolved spectra of the $\tilde{A}^1\Pi_u - \tilde{X}^1\Sigma_g^+$ transition origin band have been recorded by cavity ring-down spectroscopy, yielding accurate spectroscopic constants for all six isotopologues [23]. More detailed spectroscopic ground state information of ^{13}C-containing C_3 has become available from high-resolution rovibrational studies [20,26,29,41]. In 1993, Moazzen-Ahmadi et al. studied the ν_3 fundamentals of $^{13}C_3$ and of $^{13}C^{12}C^{12}C$, and the $\nu_3 + \nu_2 - \nu_2$ sequence band of $^{13}C_3$ around 5 μm [29]. In 2013, Krieg et al. recorded the $\nu_3 + \nu_1$ band of $^{12}C_3$, $^{13}C^{12}C^{12}C$ and $^{12}C^{13}C^{12}C$, and the $\nu_3 + \nu_2 + \nu_1 - \nu_2$ band of $^{12}C_3$ around 3 μm [26]. These bands have been analyzed together with the bands recorded by Moazzen-Ahmadi *et al.* [29], resulting in accurate molecular parameters for $^{12}C_3$, $^{13}C^{12}C^{12}C$ and $^{12}C^{13}C^{12}C$ isotopologues [26]. Later, the ν_2 fundamental bands of the six isotopologues in the far-IR region were studied in detail by terahertz spectroscopy in Ref. [20]. Spectroscopic constants were obtained and the C-C bond length was derived experimentally for each isotopologue. Furthermore, the precise line positions led to the detection of $^{13}C^{12}C^{12}C$ and $^{12}C^{13}C^{12}C$ towards Sgr B2(M) [17]. Besides all these experimental studies, important contributions came from precise theoretical work. State-of-art theoretical studies of C_3 have predicted molecular constants for several rovibrational levels in the $\tilde{X}^1\Sigma_g^+$ state for all isotopologues [41], that are in good agreement with experimental high-resolution spectroscopic values [20,22,25–27,29,35].

The study of C_3 isotopologues is also important from a chemical dynamics perspective. It is known that at low temperature the isotope ratio of molecular carbon can be significantly shifted due to small zero-point energy differences between reactants and products [42]. The observation of C_3 isotope ratios offers a useful way to characterize the involved formation pathways. In addition to rovibrational transitions in the IR region, the $\tilde{A}^1\Pi_u - \tilde{X}\ ^1\Sigma_g^+$ transition of ^{13}C-substituted C_3 provides another independent method to detect them, specifically in diffuse clouds where the light from background stars can be used to observe C_3 in direct absorption. However, to the best of our knowledge, $\tilde{A}^1\Pi_u - \tilde{X}^1\Sigma_g^+$ detections of C_3 isotopologues have been limited to the origin band [21,23]. In part this is due to severe overlap of ^{13}C-containing C_3 transitions by the stronger $^{12}C_3$ features. In this work, we performed a high-resolution spectroscopic survey of the $\tilde{A}^1\Pi_u - \tilde{X}^1\Sigma_g^+$ transition of $^{13}C^{12}C^{12}C$ and $^{12}C^{13}C^{12}C$ to obtain accurate transition frequencies and constants that can be be used to guide astronomical observations. To find $^{13}C^{12}C^{12}C$ and $^{12}C^{13}C^{12}C$ transitions that are less blended by $^{12}C_3$, all the vibrational modes in the $\tilde{A}^1\Pi_u$ state are covered. In total, thirteen vibronic bands have been recorded for these two isotopologues at a spectral resolution of ~0.02 cm^{-1}, allowing us to determine accurate molecular constants for the vibronic levels in the $\tilde{A}^1\Pi_u$ state via rotational analyses.

2. Experiment

The experiment was performed on the laser-induced fluorescence (LIF) spectrometer [43–45] in combination with a pulsed DC discharge source [46]. A gas mixture of 0.3% acetylene diluted in argon with ^{13}C at its natural abundance of about 1% was used to produce the ^{13}C mono-substituted C_3 molecules. The gas mixture with a stagnation pressure of ~6 bar was expanded into a high vacuum chamber through a pulsed valve (General Valve, Serial 9). Gas pulses of typically 200 μs were used and at a repetition rate of

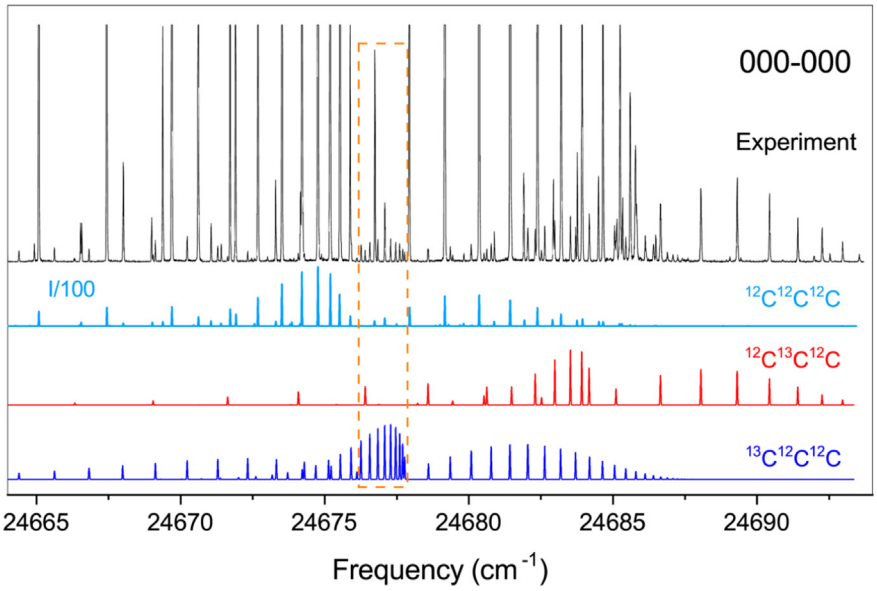

Fig. 1. The 000-000 Π_u- Σ_g^+ origin band. Upper black trace is the recorded LIF spectrum, with $^{12}C_3$ transitions being truncated. Lower traces are simulated spectra, with cyan for $^{12}C_3$, red for $^{12}C^{13}C^{12}C$ and blue for $^{13}C^{12}C^{12}C$. Note that for $^{12}C_3$ the simulated intensity is divided by 100, which is applied to all the following figures. A Gaussian linewidth of 0.023 cm^{-1} and a rotational temperature of ~30 K are used in the spectral simulations of $^{12}C^{13}C^{12}C$ and $^{13}C^{12}C^{12}C$. The orange rectangle region is displayed enlarged in Fig. 2.

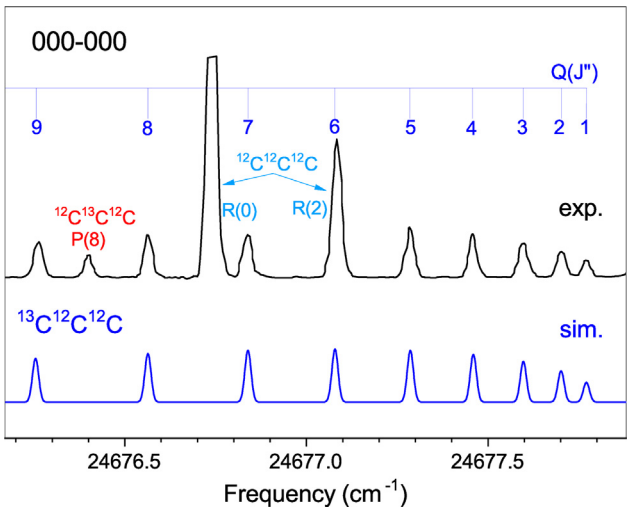

Fig. 2. Zoomed-in 000–000 band spectrum in the $^{13}C^{12}C^{12}C$ Q-branch region as marked by the orange rectangle in Fig. 1. The rotational assignments of $^{13}C^{12}C^{12}C$ are given by blue thin sticks on top of the experimental spectrum. The rotational assignments of $^{12}C_3$ and $^{12}C^{13}C^{12}C$ are given by cyan and red color.s, respectively.

10 Hz. Two stainless steel rods, acting as the electrodes, were placed with their polished flat heads opposite to each other, ~1.5 mm downstream from the nozzle orifice and perpendicular to the jet expansion. High voltage pulses (~−2000 V, 10 μs) were applied to one of the electrodes to initiate the gas discharge, while the other was grounded. A wavelength tunable laser beam was aligned perpendicularly crossing the gas jet about 30 mm away from the electrodes. Fluorescent emissions from excited C_3 molecules were collected by a telescope lens system and detected by a photomultiplier tube (PMT) (Hamamatsu, R928). A 400 ±20 nm bandpass filter (Thorlabs, FB400-40) was mounted between the lens and PMT to decrease the discharge scatter. Moreover, fluorescence was collected within a time gate width of 20 ns at a delay time of about 30 ns relative to the laser pulse. A laser excitation spectrum was recorded by measuring the overall fluorescence intensity as a function of the continuously tuned laser wavelength.

The narrowband light was generated by a home-made single-longitude-mode optical parametric oscillator (SLM-OPO) which was pumped by the second harmonic output (532 nm) of an injection-seeded Nd:YAG laser (Spectra-physics, Lab-190) [47]. The signal output of the OPO, continuously tunable in the 700–1000 nm region, had a bandwidth of 0.004 cm^{-1}. A KDP (KH_2PO_4, Castech) crystal was used for frequency doubling of the signal output of the OPO to obtain tunable radiation in the 350–450 nm region. During a running experiment, the frequency of the signal output was calibrated online by a wavelength meter (High Finesse, WS7-60). The wavelength meter was self-calibrated with a stabilized He-Ne laser, providing an absolute accuracy of ~0.002 cm^{-1}. For all the vibronic bands, the spectral linewidths (full width at half maximum) of fully resolved rotational lines are found to be narrower than 0.023 cm^{-1}, while individual line positions can be determined with an accuracy of ~0.003 cm^{-1}.

3. Results and analysis

In a range of 378–406 nm, thirteen vibronic bands of the $\tilde{A}^1\Pi_u - \tilde{X}^1\Sigma_g^+$ transition have been recorded for $^{13}C^{12}C^{12}C$ and $^{12}C^{13}C^{12}C$, all of which are assigned as transitions from the ground state (000) levels to the different vibrational quanta of the (anti) symmetric stretch and bending vibration in the upper electronic state. Among them, eight bands belong to the $^{13}C^{12}C^{12}C$ isotopologue, whose upper vibronic levels and term energies are summarized in Table 1. The other five bands belong to $^{12}C^{13}C^{12}C$ and are summarized in Table 2. The high-resolution LIF spectra are displayed in Figs. 1–10, details of which are given in the subsections below. Because no ^{13}C enriched precursor gas was used, the recorded spectra contained very strong lines of the main isotopologue $^{12}C_3$ (e.g. Fig. 1). Despite some spectral overlap, this offered a good guidance for vibrational assignments for the two isotopologues, $^{13}C^{12}C^{12}C$ and $^{12}C^{13}C^{12}C$, since the vibronic bands of $^{12}C_3$-have been already well studied [3,11,19].

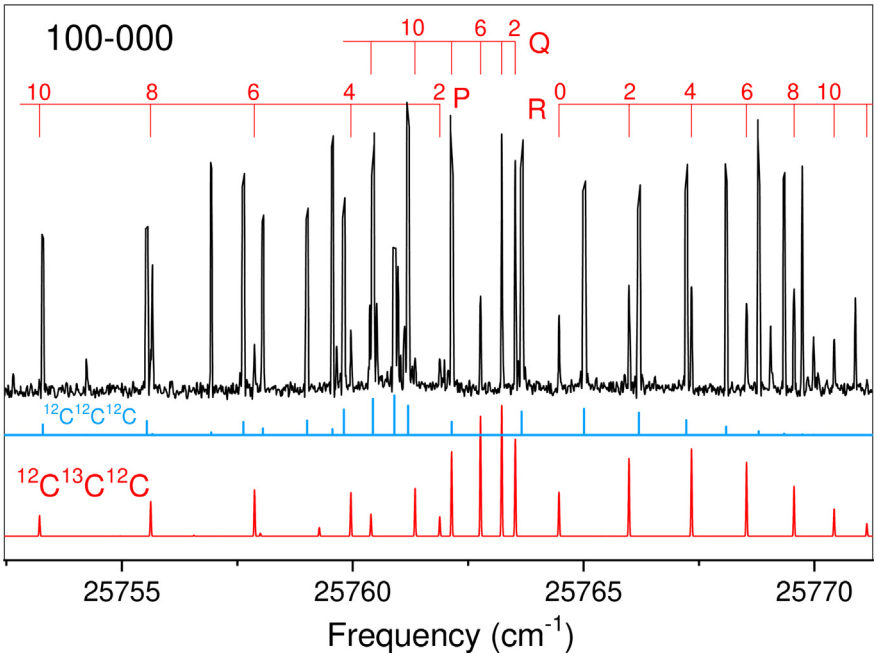

Fig. 3. The 100–000 Π_u- Σ_g^+ band. Upper black trace is the recorded LIF spectrum, with $^{12}C_3$ transitions being truncated. Lower traces are simulated spectra, with cyan for $^{12}C_3$ and red for $^{12}C^{13}C^{12}C$. A Gaussian linewidth of 0.02 cm^{-1} and a rotational temperature of ~30 K are used in the spectral simulations.

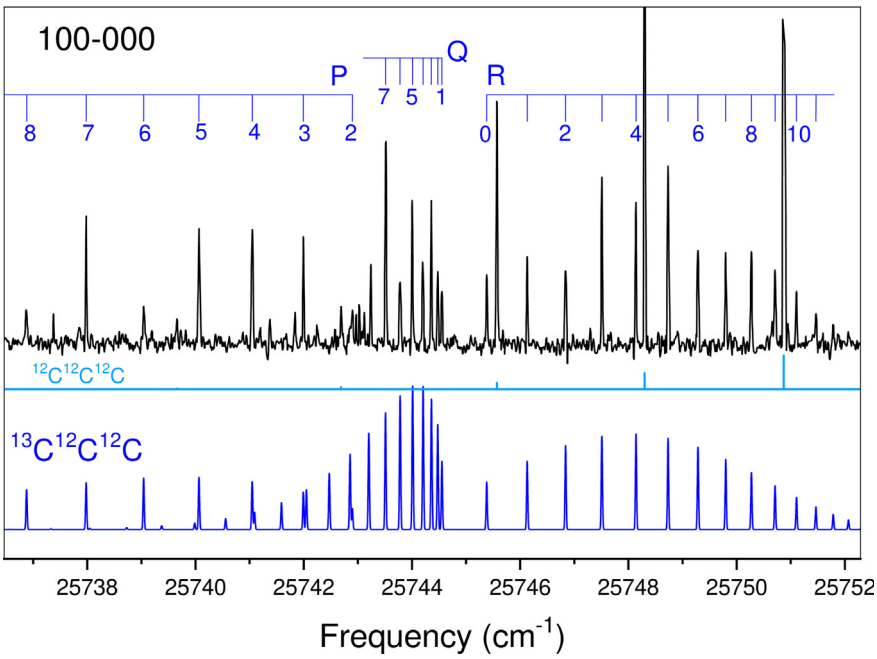

Fig. 4. The experimental (upper black trace) and simulated (lower blue trace) high-resolution spectra of $^{13}C^{12}C^{12}C$ 100–000 band. The rotational assignments are given by thin sticks on top of the experimental spectrum. A Gaussian linewidth of 0.02 cm^{-1} and a rotational temperature of ~30 K are used in the spectral simulation. Middle cyan trace is the simulated spectrum of $^{12}C_3$.

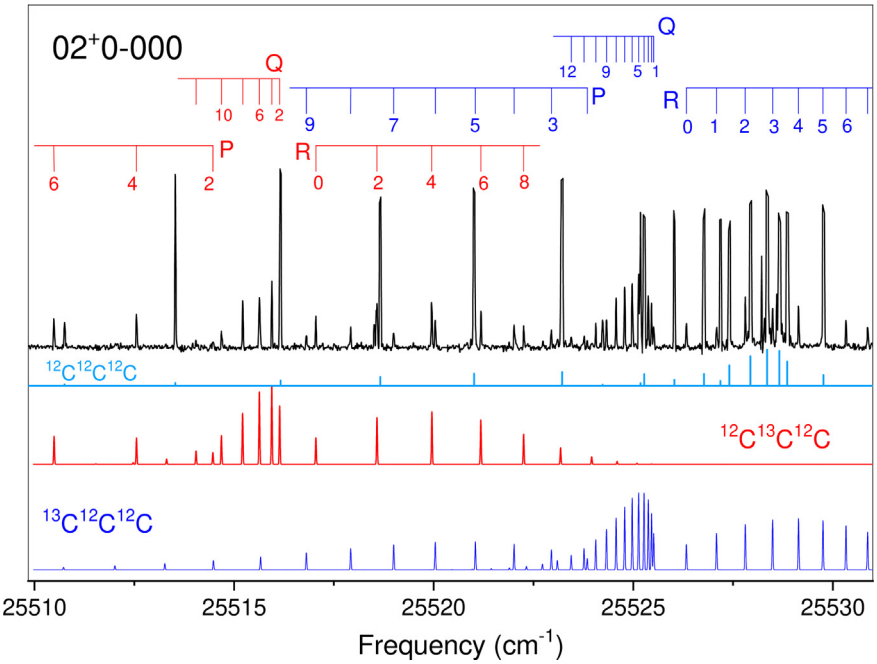

Fig. 5. The 02^+0–000 Π_u^+- Σ_g^+ band. Upper black trace is the recorded LIF spectrum, with $^{12}C_3$ transitions being truncated. The rotational assignments of $^{12}C^{13}C^{12}C$ and $^{13}C^{12}C^{12}C$ are given by red and blue thin ticks, respectively, on the top of the spectrum. Lower traces are simulated spectra, with cyan for $^{12}C_3$, red for $^{12}C^{13}C^{12}C$ and blue for $^{13}C^{12}C^{12}C$. A Gaussian linewidth of 0.02 cm^{-1} and a rotational temperature of ~30 K are used in the spectral simulations.

3.1. The 000–000 band

Fig. 1 (upper black trace) shows the recorded origin band of $\tilde{A}^1\Pi_u - \tilde{X}^1\Sigma_g^+$ transition for the $^{12}C_3$, $^{13}C^{12}C^{12}C$ and $^{12}C^{13}C^{12}C$ isotopologues. The rotational lines of $^{12}C_3$ have been truncated. In addition to their higher intensity, $^{12}C_3$ lines are further identified using the conclusions from previous studies [23,37,39]. The weaker lines around 24678 cm^{-1} and 24690 cm^{-1} belong to the Q-branch of $^{13}C^{12}C^{12}C$ and R-branch of $^{12}C^{13}C^{12}C$, respectively. The adjacent line intervals of $^{13}C^{12}C^{12}C$ are obviously narrower than that of $^{12}C^{13}C^{12}C$, because the substitution by ^{13}C at terminal position breaks central symmetry in this isotopologue whereby both even and odd J'' levels in $\tilde{X}^1\Sigma_g^+$ have equal and non-zero statistics weight. By contrast, in $^{12}C^{13}C^{12}C$ the substitution keeps central symmetry and gives a zero statistics weight to the odd J'' rotational

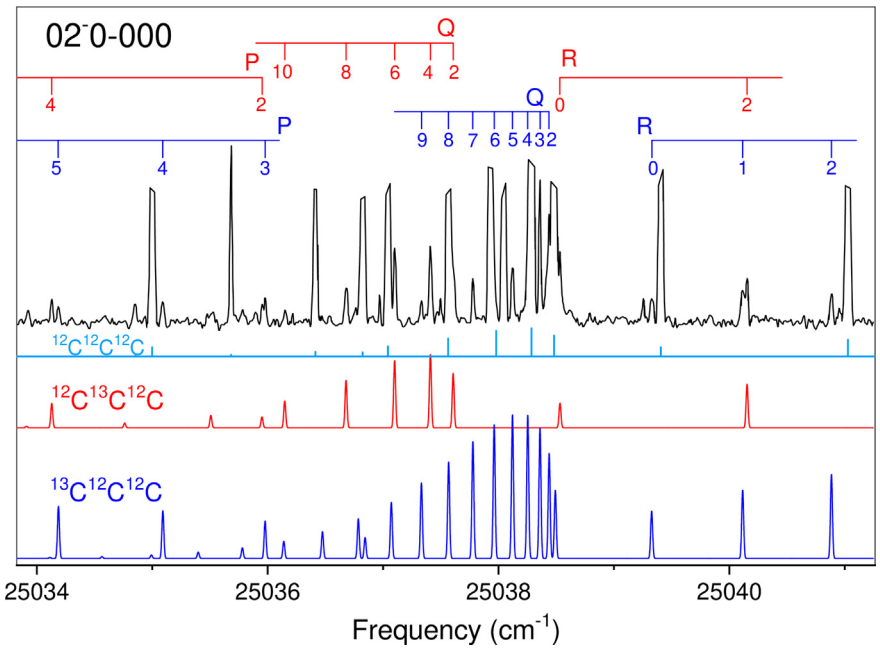

Fig. 6. The 02⁻0–000 $\Pi_u^- - \Sigma_g^+$ band. Upper black trace is the recorded LIF spectrum, with $^{12}C_3$ transitions being truncated. The rotational assignments of $^{12}C^{13}C^{12}C$ and $^{13}C^{12}C^{12}C$ are given by red and blue thin ticks, respectively, on the top of the spectrum. Lower traces are simulated spectra, with cyan for $^{12}C_3$, red for $^{12}C^{13}C^{12}C$ and blue for $^{13}C^{12}C^{12}C$. A Gaussian linewidth of 0.02 cm^{-1} and a rotational temperature of ~30 K are used in the spectral simulations.

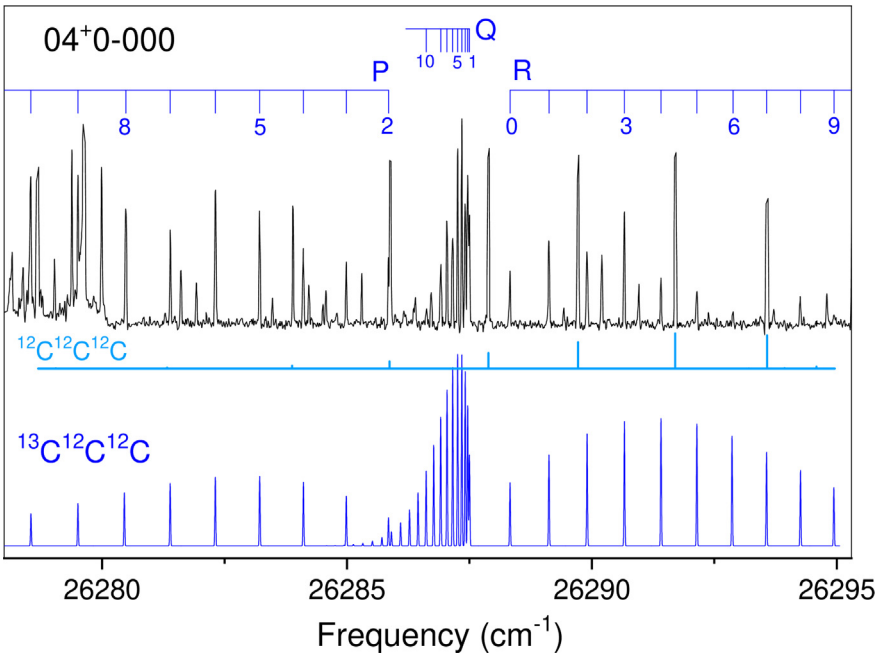

Fig. 7. The experimental (upper black trace) and simulated (lower blue trace) spectra of $^{13}C^{12}C^{12}C$ 04^+0–000 band. The rotational assignments are given by blue thin sticks on top of the experimental spectrum. A Gaussian linewidth of 0.02 cm^{-1} and a rotational temperature of ~30 K are used in the spectral simulation. Middle cyan trace is the simulated spectrum of $^{12}C_3$.

levels in the $\tilde{X}^1\Sigma_g^+$ state. It should be mentioned that a centro-symmetric geometry also applies to the $^{13}C^{12}C^{13}C$ and $^{13}C^{13}C^{13}C$ isotopologues, however, the non-zero spin of ^{13}C (Fermi statistics) only weakens the lines originating from even J'' rotational levels in the $\tilde{X}^1\Sigma_g^+$ state, which can be seen clearly in the spectra recorded by Haddad et al. (Figs. 2 and 3) who used ^{13}C enriched precursor material [23]. The different behaviours of rotational structure support the spectral carrier attributions. Besides, the much lower abundance of the di- or tri- ^{13}C-substituted isotopologues makes them undetectable for the present experimental conditions.

The rotational analysis was performed using PGOPHER software and an $\mathbf{N^2}$ form Hamiltonian for a linear molecule [48]. For the lower Σ symmetry state, the rotational energy is expressed as

$$F(J) = BJ(J+1) - DJ^2(J+1)^2 + HJ^3(J+1)^3 \quad (1)$$

where B is the rotational constant, and D and H are the quartic and sextic centrifugal distortion constants, respectively. For the upper Π symmetry vibronic state, the rotational energy is expressed as

$$F_v(J) = T_v + B_vJ(J+1) - D_vJ^2(J+1)^2 \pm (1/2)q_vJ(J+1) \quad (2)$$

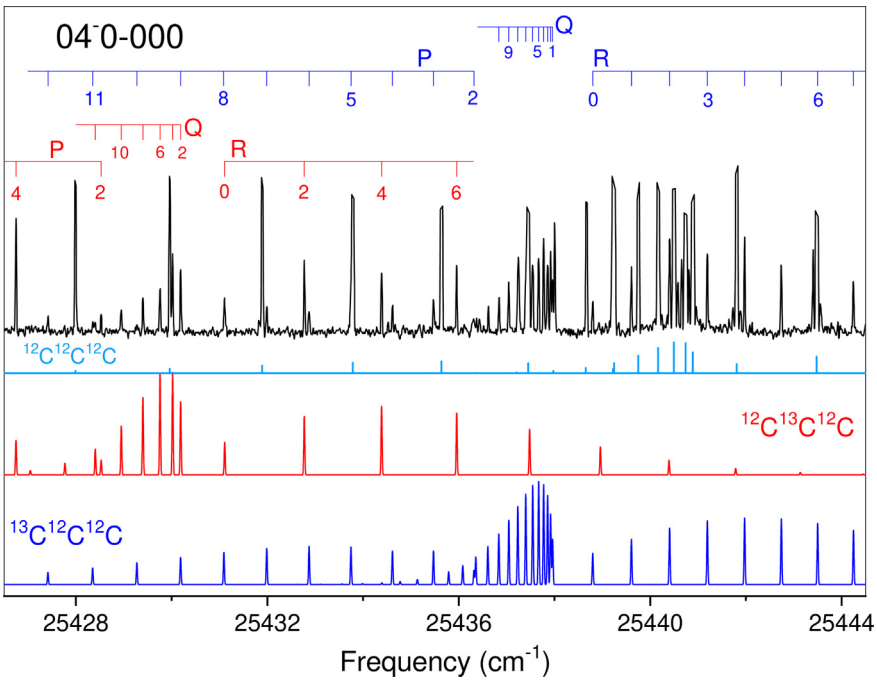

Fig. 8. The 04⁻0–000 Π_u^-- Σ_g^+ band. Upper black trace is the recorded LIF spectrum, with $^{12}C_3$ transitions being truncated. The rotational assignments of $^{12}C^{13}C^{12}C$ and $^{13}C^{12}C^{12}C$ are given by red and blue thin ticks, respectively, on the top of the spectrum. Lower traces are simulated spectra, with cyan for $^{12}C_3$, red for $^{12}C^{13}C^{12}C$ and blue for $^{13}C^{12}C^{12}C$. A Gaussian linewidth of 0.02 cm^{-1} and a rotational temperature of ~30 K are used in the spectral simulations.

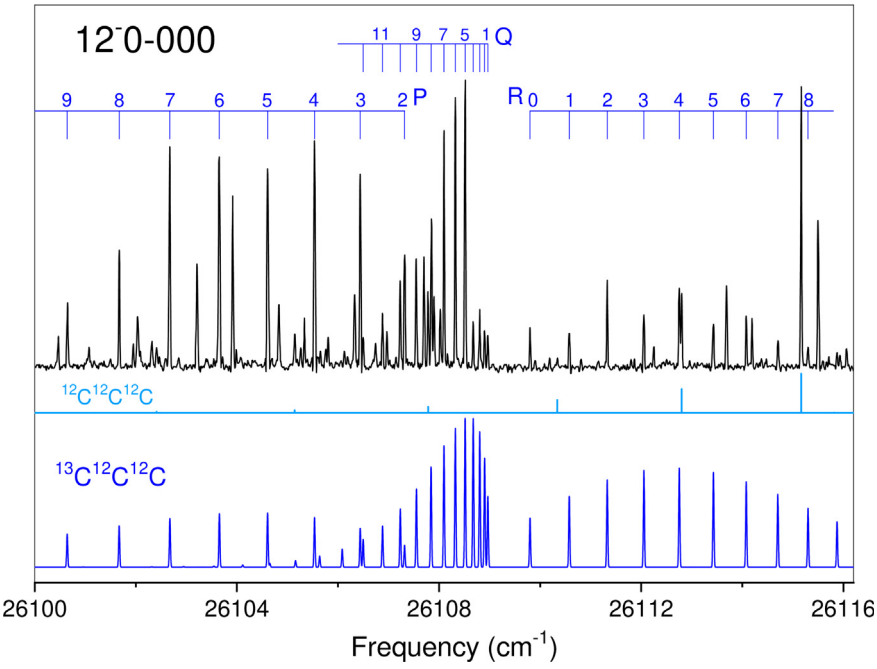

Fig. 9. The experimental (upper black trace) and simulated (lower blue trace) spectra of $^{13}C^{12}C^{12}C$ 12^-0–000 band. The rotational assignments are given by blue thin sticks on top of the experimental spectrum. A Gaussian linewidth of 0.02 cm^{-1} and a rotational temperature of ~30 K are used in the spectral simulation. Middle cyan trace is the simulated spectrum of $^{12}C_3$.

where T_v is the vibronic term energy, q_v is the Λ-doubling parameter, and the plus and minus signs refer to states with *f*and *e*parity, respectively. It is found that the sextic centrifugal distortion term for the $\tilde{A}^1\Pi_u$ state is not necessary to reproduce the observed spectra. The rotational assignments are made by using combination differences in the lower state, that is, the frequency differences between R(J'') and P($J''+2$) lines are determined only by the lower rovibrational levels, which can be calculated from the accurate constants available from Ref.[20]. In total, 44 transitions with J'' levels up to 21 have been recorded for $^{13}C^{12}C^{12}C$ and 32 lines with J'' levels up to 22 have been observed for $^{12}C^{13}C^{12}C$. Part of the assignments are depicted in Fig.2, while all the assignments

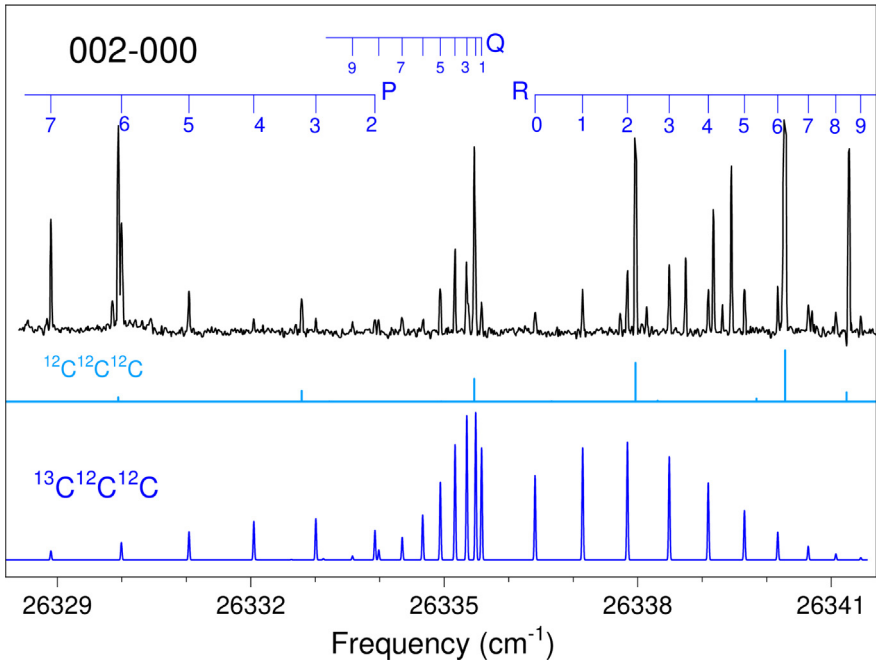

Fig. 10. The experimental (upper black trace) and simulated (lower blue trace) spectra of $^{13}C^{12}C^{12}C$ 002–000 band. The rotational assignments are given by blue thin sticks on top of the experimental spectrum. A Gaussian linewidth of 0.02 cm^{-1} and a rotational temperature of ~30 K are used in the spectral simulation. Middle cyan trace is the simulated spectrum of $^{12}C_3$.

together with the line positions are collected in the supplementary materials. By examination of the combination differences in the lower state [20], an absolute accuracy of ~0.003 cm^{-1} is obtained for the observed lines, which is a significant improvement compared with existing data with an accuracy of ~0.04 cm^{-1} [23]. To obtain more accurate spectroscopic constants for the $\widetilde{A}(0,0,0)$ level, a least-squares fit procedure is performed in the PGOPHER software [48]. In the fit, constants for the $\widetilde{X}(0,0,0)$ state are fixed to the values reported by Breier et al.[20], while the constants of the $\widetilde{A}(0,0,0)$ state are varied simultaneously until all observation-calculation (obs.–cal.) deviations of assigned transition lines agree well with our experimental uncertainty. The root mean square of the fit is ~0.002 cm^{-1} (1σ), indicating an excellent agreement between the observed and calculated line positions. The spectroscopic constants determined from the fit for the $\widetilde{A}(0,0,0)$ state are summarized in Tables 1,2 for $^{13}C^{12}C^{12}C$ and $^{12}C^{13}C^{12}C$, respectively. The simulated spectra using these parameters are shown in Fig. 1 and a zoom-in of $^{13}C^{12}C^{12}C$ Q-branch is displayed in Fig. 2.

Table 1
Spectroscopic constants for the $\tilde{A}^1\Pi_u$ (v_1, v_2^l, v_3) state of $^{13}C^{12}C^{12}C$ (in cm^{-1}).[a]

Vibronic[b]	T_v	B_v	q_v	D_v
000	24677.80493(31)	0.3964097(49)	3.05(54) e-5	1.95(11) e-7
100	25744.59273(53)	0.394225(22)	−2.83(21) e-4	6.8(15) e-7
02^+0	25525.53859(44)	0.398065(17)	−4.3989(66) e-3	1.07(11) e-6
02^-0	25038.51847(46)	0.4022105(92)	3.570(12) e-3	–
04^+0[c]	26287.5179(11)	0.405194(63)	5.06(33) e-4	−3.94(63) e-6[c]
04^-0	25437.98129(46)	0.406119(19)	5.5167(90) e-3	1.70(14) e-6
12^-0	26108.9992(16)	0.399211(26)	3.414(35) e-3	–
002	26335.62507(39)	0.3911465(80)	5.88(11) e-4	–

[a]Numbers in parentheses are 1σ uncertainties in units of the least significant digits. Current experimental accuracy is ~0.003 cm^{-1}.
[b]All vibronic levels are observed through fundamental transitions.
[c]Perturbations are observed for this level and the constants are effective ones. See text for details.

Table 2
Spectroscopic constants for the $\tilde{A}^1\Pi_u$ (v_1, v_2^l, v_3) state of $^{12}C^{13}C^{12}C$ (in cm^{-1}).[a]

Vibronic[b]	T_v	B_v	q_v	D_v
000	24684.27839(36)	0.4123446(39)	3.181(16) e-4	2.494(78) e-7
100	25763.64674(66)	0.409636(21)	5.662(86) e-4	7.2(12) e-7
02^+0[c]	25516.22818(48)	0.4136188(95)	−4.989(15) e-3	–
02^-0	25037.69340(59)	0.418136(10)	4.086(14) e-3	–
04^-0	25430.26012(65)	0.421380(27)	6.148(25) e-3	7.2(20) e-7

[a] Numbers in parentheses are 1σ uncertainties in units of the least significant digits. Current experimental accuracy is ~0.003 cm^{-1}.
[b]All vibronic levels are observed through fundamental transitions.
[c]Perturbations are observed for this level and the constants are effective ones. See text for details.

3.2. The 100–000 band

The 100–000 (Π_u- Σ_g^+) band of the main isotopologue $^{12}C_3$ has been studied previously [3,11,19]. The same band recorded here is shown in Fig. 3. The top of each line has been truncated to focus on the weaker ^{13}C-containing C_3 isotopologue signals. The band origin, ~25761 cm^{-1}, and line positions are in good agreement with previous work [3,11,19]. Also shown in Fig. 3 is the 100–000 (Π_u- Σ_g^+) band of $^{12}C^{13}C^{12}C$ whose origin is around 25764 cm^{-1}. The R-branch develops to the blue side while the Q- and P-branches degrade to the red side. The interval between the first two lines in the R-branch is ~1.51 cm^{-1}, which value is very similar to that of $^{12}C_3$ (~1.52 cm^{-1}). This is consistent with the ^{12}C ($I = 0$) spin-statistics, and serves as evidence that attributes $^{12}C^{13}C^{12}C$ as the carrier of this band.

Since the spectroscopic constants in the ground state of $^{12}C^{13}C^{12}C$ have been accurately determined in Ref. [20], combination differences in the ground state can be used to help the rotationally assignments of the 100–000 band. In total, 18 transitions with J'' up to 12 have been assigned for this band (Fig. 3). The assignments and corresponding transition frequencies are given in the supplementary materials. The combination differences R(J'') – P($J''+2$) determined from the assigned lines agree very well with those derived from Ref. [20]. The derivations are within 0.003 cm^{-1} for J'' levels up to 12. This further confirms $^{12}C^{13}C^{12}C$ as the carrier of this band. A least-squares fit procedure was performed in PGOPHER [48] to obtain spectroscopic constants for the $\widetilde{A}$(1,0,0) state. Eqs. 1 and 2 are used to express the lower and upper level energies in the 100–000 band, respectively. In the fit, constants for the $\widetilde{X}$(0,0,0) state are fixed to the values reported by Breier et al. [20], while the constants of the $\widetilde{A}$(1,0,0) state are varied simultaneously until all obs.–cal. deviations of assigned transition lines agree with our experimental uncertainty. In the final fit, a root mean square error of ~0.002 cm^{-1} (1σ) was obtained. The resulting constants for the $\widetilde{A}$(1,0,0) state are summarized in Table 1. It should be noted that the constants for the $\widetilde{A}$(1,0,0) state of $^{12}C^{13}C^{12}C$ are reported for the first time. The simulated spectrum using these constants is shown in Fig. 3 (lower trace).

Fig. 4 (upper black trace) displays the observed 100–000 (Π_u- Σ_g^+) band of $^{13}C^{12}C^{12}C$ whose origin is about 25745 cm^{-1}. This band locates in the well separated P-branch lines of $^{12}C_3$ 100–000 band, and therefore, its profile is ready to be recognized. The adjacent line spacing is much narrower than that of $^{12}C_3$ and $^{12}C^{13}C^{12}C$. Specifically, the interval between the first two transitions in the R-branch is ~0.75 cm^{-1}, roughly half of that of $^{12}C^{13}C^{12}C$ (~1.51 cm^{-1}). This is because non-centrosymmetry structure in $^{13}C^{12}C^{12}C$ leads to equal statistic weight for both the even and odd J'' levels in the ground state. With a spectral resolution of 0.023 cm^{-1}, the rotational structures are fully resolved, rendering the assignments straightforward. In total, 27 transitions with J'' levels up to 11 have been assigned for this band (Fig. 4). The assigned lines and corresponding line positions are provided in the supplementary materials. The combination differences R(J'') – P($J''+2$) determined from the assigned lines agree within 0.003 cm^{-1} with those of $^{13}C^{12}C^{12}C$ derived from Ref. [20], which confirms the spectral carrier as $^{13}C^{12}C^{12}C$. The spectroscopic constants for $^{13}C^{12}C^{12}C$ $\widetilde{A}$(1,0,0) state in Table 1 were determined from a least-squares fit of all the transition frequencies extracted from the assigned lines. The root mean square error was found to be ~0.002 cm^{-1} (1σ) in the final fit. The simulated spectrum using the obtained constants is displayed in Fig. 4 (lower trace).

3.3. The 020–000 band

Due to the interaction between bending vibration and electron motion in the $\tilde{A}^1\Pi_u$ electronic state, C_3 exhibits a Renner-Teller effect, i.e. the bending vibration level splits into several components distinguished by the quantum number K of the total angular momentum along the internuclear axis ($K = |l \pm \Lambda|$). Here for the $\widetilde{A}$(0,2,0) level, it splits into the three components, Π_u^+, Φ_u, and Π_u^-(see Fig. 9 in Ref. [3]). Because the $\widetilde{X}$(0,0,0) state is of Σ_g^+ symmetry, two vibronic bands are allowed in the 020–000 transition, Π_u^+- Σ_g^+ and Π_u^-- Σ_g^+, denoting as 02$^+$0–000 and 02$^-$0–000, respectively. These two bands for the main isotopologue $^{12}C_3$ have been reported in Refs. [3,11,19,38]. Guided by these studies, the 02$^+$0–000 and 02$^-$0–000 bands have been observed for ^{13}C mono-substituted isotopologues $^{13}C^{12}C^{12}C$ and $^{12}C^{13}C^{12}C$.

Fig. 5 depicts the recorded LIF spectrum of the 02$^+$0–000 (Π_u^+- Σ_g^+) bands for $^{12}C_3$, $^{13}C^{12}C^{12}C$ and $^{12}C^{13}C^{12}C$. The $^{12}C_3$ 02$^+$0–000 band origin is ~25529 cm^{-1}, consistent with previous work [3,11,19]. On the red side, around 25526 cm^{-1} and 25516 cm^{-1} we find the band origins of $^{13}C^{12}C^{12}C$ and $^{12}C^{13}C^{12}C$, respectively. Again, the adjacent line spacing of $^{13}C^{12}C^{12}C$ is much narrower than the other two because both the even and odd J'' levels in the ground state have non-zero statistic weight. The spectral carriers are further confirmed by examination of the lower state combination differences as mentioned in subSection 3.2.

In total, 32 transitions with J''=0–12 were assigned for $^{13}C^{12}C^{12}C$ and 14 transitions with J'' levels up to 12 were assigned for $^{12}C^{13}C^{12}C$. The assignments together with the transition frequencies for $^{13}C^{12}C^{12}C$ and $^{12}C^{13}C^{12}C$ are summarized in the supplementary materials. To obtain the molecular parameters for the $\widetilde{A}$(0,2$^+$,0) state, least-squares fits of the assigned line positions were performed by using the linear Hamiltonian embedded in PGOPHER [48]. The resulting constants of $^{13}C^{12}C^{12}C$ and $^{12}C^{13}C^{12}C$ are given in Tables 1,2, respectively.

From the rotational analysis, it is found that, in the 02$^+$0–000 band of $^{12}C^{13}C^{12}C$, the P(6) and R(4) transitions are observed to be redshifted by ~0.01 cm^{-1} from the calculated values. Since both these two transitions end at the same level J'=5 in the $\widetilde{A}$(0,2$^+$,0) state, it is likely that this level is weakly perturbed. Similarly, the levels J'=7 and 8 are found to deviate from the calculated positions by 0.006 cm^{-1} which is about twice the current experimental accuracy (0.003 cm^{-1}). These discrepancies can not be caused by inaccurate constants because other lines are well reproduced. A search for the possible perturber transitions was negative. As a result, these perturbed transitions are excluded from the final fit and the constants for the $^{12}C^{13}C^{12}C$ $\widetilde{A}$(0,2$^+$,0) state in Table 2 are effective ones, reproducing all observed transitions with exception of the perturbed ones. For the $^{13}C^{12}C^{12}C$ isotopologue, no such perturbations are observed.

As shown in Fig. 6, around the crowded Q- branch of $^{12}C_3$ 02$^-$0–000 (Π_u^-- Σ_g^+) band (~25038 cm^{-1}), the 02$^-$0–000 bands of $^{13}C^{12}C^{12}C$ and $^{12}C^{13}C^{12}C$ are observed. Some transitions of the latter two are blended by signals of the main isotopologue. To assign the rovibronic transitions, such as of $^{13}C^{12}C^{12}C$, a preliminary spectrum was simulated in PGOPHER [48] by using the constants reported in Ref. [20] for the ground state and estimated constants for the $\widetilde{A}$(0,2$^-$,0) state. Then, some resolved P- and R-lines were tentatively assigned, followed by a fit to optimise the upper state constants. As a result, more lines could be assigned. This self guiding procedure was repeated and after several trials, 26 transitions including the blended ones were assigned for this band (Fig. 6).

The lines are collected in the supplementary materials. After that, the constants for the $\widetilde{A}(0,2^-,0)$ state (Table 1) were determined through the least-squares fit of the transition frequencies of the assigned lines. It should be pointed out that this method can be applied because the spectral resolution is high enough such that reasonable constants can be determined from less assigned lines. Clearly, this procedure only works as this band is free of (severe) perturbations. Using the same method, fifteen transitions were assigned for $^{12}C^{13}C^{12}C$ 02^-0–000 band (Fig. 6). The line list is summarized in the supplementary materials and the constants determined from the fit are given in Table 2.

3.4. The 040–000 band

Because of the Renner-Teller interaction the bending excited level, $\widetilde{A}(0,4,0)$, splits into five components, Π_u^+, Φ_u^+, H_u, Φ_u^- and Π_u^-, among which, the two states Π_u^+ and Π_u^- are accessible from the $\widetilde{X}(0,0,0)$ Σ_g^+ state. In the present work, the Π_u^+- Σ_g^+ or 04^+0–000 band has been recorded only for $^{13}C^{12}C^{12}C$ and the Π_u^-- Σ_g^+ or 04^-0–000 band has been recorded for both $^{13}C^{12}C^{12}C$ and $^{12}C^{13}C^{12}C$.

Fig. 7 displays the LIF spectrum of the $^{13}C^{12}C^{12}C$ 04^+0–000 band. The origin locates at ~26287.5 cm^{-1}, about 10 cm^{-1} lower than that of $^{12}C_3$. The adjacent line intervals of $^{13}C^{12}C^{12}C$ are smaller as both even and odd J'' levels in the ground state have non-zero statistic weight. Following combination differences in the $\widetilde{X}(0,0,0)$ state [20], rotational assignments were made and the spectral carrier was confirmed. In total, 26 transitions including J''= 0–11 were assigned, whose assignments are shown in Fig. 7 and the line positions are collected in the supplementary materials. The combination differences $R(J'') - P(J''+2)$ determined from the assigned lines agree within 0.004 cm^{-1} with those of $^{13}C^{12}C^{12}C$ derived from Ref. [20].

In an attempt to derive the $\widetilde{A}(0,4^+,0)$ state constants, a meaningless negative centrifugal distortion constant D was obtained. Further trials show that positive D values resulted in obs. -cal. errors that are significantly larger than the experimental accuracy. The discrepancies show a regular pattern that gradually increases as J moves to larger values. A trial of adding the sextic centrifugal distortion term, $HJ^3(J+1)^3$, to Eq. 2 did not change the pattern. Instead, a negative D value decreases the discrepancies to within the current experiment accuracy. These results suggest that J dependent perturbations take place in the $\widetilde{A}(0,4^+,0)$ state of $^{13}C^{12}C^{12}C$. Due to the lack of perturber transitions, a set of effective parameters (Table 1) is derived from least-squares fit by using Eq. 2. The inclusion of a negative D-constant allows to reproduce the observed lines quite well, but obviously should only be used with care when predicting line positions beyond those recorded here.

In Fig. 8, the relative broader and flat-top lines belong to the 04^-0–000 (Π_u^-- Σ_g^+) band of the main isotopologue $^{12}C_3$. The band origin is around 25441 cm^{-1}, and this value is in good agreement with previous work [3,11,19]. At the lower energy side, around 25438 cm^{-1} and 25430 cm^{-1} are the 04^-0–000 (Π_u^-- Σ_g^+) bands of $^{13}C^{12}C^{12}C$ and $^{12}C^{13}C^{12}C$, respectively. These three spectra show a similar contour, that is, the Q-branch located at the spectral center develops to the red side, and the P- and R-branches degrade smoothly to red and blue sides, respectively. Again, the band of $^{13}C^{12}C^{12}C$ is more dense than the others. With the fully resolved rotational structures, the assignments were straightforward and were further confirmed by the combination differences in the ground states. In total, 30 transitions with J'' levels up to 13 have been assigned to $^{13}C^{12}C^{12}C$ and the details are given in the supplementary materials. As for $^{12}C^{13}C^{12}C$, twelve transitions with J'' levels up to 12 have been assigned and the line positions are given in the supplementary materials. Some of the assignments are shown in Fig. 8. No perturbations have been observed for the $\widetilde{A}(0,4^-,0)$ levels of $^{13}C^{12}C^{12}C$ and $^{12}C^{13}C^{12}C$ extending beyond the current experimental accuracy (0.003 cm^{-1}). Accurate constants for the upper states were consequently determined through least squares fits of the line positions. The results of $^{13}C^{12}C^{12}C$ and $^{12}C^{13}C^{12}C$ are summarized in Tables 1,2, respectively. The simulated spectra using the obtained constants are displayed in Fig. 8.

3.5. The 12^-0–000 band

Fig. 9 shows the recorded 12^-0–000 (Π_u^-- Σ_g^+) spectrum of $^{13}C^{12}C^{12}C$. The band origin is about 26109 cm^{-1}, which is ~18 cm^{-1} lower than for the corresponding band of the main isotopologue $^{12}C_3$ [3,11,19]. As in parts of the involved frequency domain ($\leqslant$26180.5 cm^{-1}, roughly Q(5)) no $^{12}C_3$ signals show up, it was possible to use a higher laser power. Based on the lower state combination differences, 31 transitions with J'' levels up to 12 were assigned for this band. The assignments are shown in Fig. 9 and the line positions are collected in the supplementary materials. Similar as aforementioned procedure, the constants for $\widetilde{A}(12^-0)$ state were determined from fitting the assigned lines and are summarized in Table 1. The obs.–cal. errors are within 0.003 cm^{-1}. The simulated spectrum using the obtained constants is shown in the lower trace of Fig. 9.

3.6. The 002–000 band

The 002–000 (Π_u- Σ_g^+) band of the main isotopologue $^{12}C_3$ has been reported around 26346 cm^{-1} [3,11,19]. At the lower frequency side, around 26335.5 cm^{-1}, the 002–000 (Π_u^-- Σ_g^+) band of $^{13}C^{12}C^{12}C$ was found in the present work (Fig. 10). The Q- and P-branches degrade to the red side while the R-branch degrades smoothly to the blue side. Both even and odd $J'' \leqslant 10$ were observed in the current spectrum. The assignments were made and confirmed with the help of combination differences, $R(J'') - P(J''+2)$, in the ground state [20]. In total, 26 transitions have been assigned, whose details are given in the supplementary materials. The spectroscopic constants for $\widetilde{A}(0,0,2)$ state were subsequently determined by a least squares fit of the observed line frequencies and the results are summarized in Table 1. The obs.–cal. errors for all the observed lines are within 0.003 cm^{-1}. The simulated spectrum using the constants is shown in the lower trace of Fig. 10.

4. Astrophysical implication

Comparing laboratory data to astronomical observations offers a powerful tool to get a better picture of the chemical processes taking place in space. This work has been at the core of Prof. Stephan Schlemmer's work [15,26] that we want to celebrate with this study on C_3 isotopologues. The current work provides accurate spectroscopic data for the $\tilde{A}\ ^1\Pi_u - \tilde{X}^1\Sigma_g^+$ optical transition of the ^{13}C mono-substituted $^{13}C^{12}C^{12}C$ and $^{12}C^{13}C^{12}C$ isotopologues. Thirteen rotationally fully resolved vibronic bands covering all the vibrational modes in the $\tilde{A}^1\Pi_u$ state have been recorded with a linewidth of 0.023 cm^{-1}, corresponding to a resolution power of $\sim 10^6$. The transition frequencies extracted from the spectra are found to be of an absolute frequency accuracy of 0.003 cm^{-1}.

So far, more than 200 molecules have been identified in the interstellar medium and circumstellar envelopes [49]. Their rela-

tive abundance and isotope ratios can vary drastically, depending on the region under investigation (see CDMS[1]). It has been shown that at low temperature the isotope ratio of molecular carbon can be significantly different from values found on Earth due to small zero-point energy differences between reactants and products [42]. Astronomical observations have found that for some carbon bearing molecules, such as HCCCN, C_3S, C_4H and so on [50,51], isotope abundances show strong dependence on the ^{13}C-substituted position, which indicates that the carbon atoms are not equivalent in their formation pathways. The observed differences are explained by a gas-grain chemical network model constructed by Furuya et al. [52]. It is confirmed that the isotope ratios of molecules, both in the gas phase and on grain surfaces, mostly depend on whether these species are formed from the carbon atom (ion) or the CO molecule. Specifically, the $^{12}C/^{13}C$ isotope ratio is larger when the species is formed from a carbon atom, while the ratio is smaller when the species is formed from a CO molecule [52].

A gas and grain warm-up model proposed by Mookerjea et al. has explained the abundance of C_3 in the warm envelopes of hot cores in a consistent manner [16]. Very recently, the detection of $^{13}C^{12}C^{12}C$ and $^{12}C^{13}C^{12}C$ along the line of sight towards Sgr B2(M) allowed to determine the $^{12}C/^{13}C$ element ratio in the C_3 molecules to be 20.5 ± 4.2 [17]. This value is in agreement with the elemental ratio of 20, typically observed in Sgr B2(M). However, it is found that the N($^{13}C^{12}C^{12}C$)/N($^{12}C^{13}C^{12}C$) ratio amounts to 1.2 ± 0.1, which is shifted from the statistically expected value of two. Giesen et al. [17] also pointed out that this finding is different from that of other molecules (such as CCH, CH_3CCH) observed in the same region since they are identical irrespective of the position of the isotope-substituted carbon atom in the molecule. It has been suggested that this discrepancy arises due to the lower zero-point energy of $^{12}C^{13}C^{12}C$, which makes position-exchange reactions converting $^{13}C^{12}C^{12}C$ to $^{12}C^{13}C^{12}C$ energetically more favourable.

However, to what extend the formation pathways contribute to the anomalous N($^{13}C^{12}C^{12}C$)/N($^{12}C^{13}C^{12}C$) ratio in Sgr B2(M) [16] remains an open question. Further observations of ^{13}C-substituted C_3 may help address this question. In addition, besides IR spectra, the $\tilde{A}^1\Pi_u - \tilde{X}^1\Sigma_g^+$ electronic transition of C_3 provides an alternative method to detect this molecule, specifically in lower density number regions such as translucent and diffuse clouds. In this regard, the accurate laboratory transition frequencies of $^{13}C^{12}C^{12}C$ and $^{12}C^{13}C^{12}C$ analysed in this work are expected to assist astronomical observations. Furthermore, the present data provide a tool to investigate isotope dependent chemistry also in translucent clouds. This may help in further constraining the conditions that determine the formation of the elusive molecules that must be the carriers of the diffuse interstellar bands. Among the thirteen vibronic bands, the 100–000, 04^+0–000 and 12^-0–000 bands of $^{13}C^{12}C^{12}C$, and the 02^+0–000, 04^-0–000 bands of $^{12}C^{13}C^{12}C$ are found to be less blended by the $^{12}C_3$ isotopologue, and therefore are more suitable to search for $^{13}C^{12}C^{12}C$ and $^{12}C^{13}C^{12}C$ in the ISM or in the comae of comets. Finally, spectroscopic constants reported in this study may also have implications in an accurate interpretation of the excited state structure of the C_3 molecule. Very recently, accurate ground state data of C_3 isotopologues have been used for a direct determination of the bond lengths, which results are in good agreement with the earlier high-level ab initio results [41]. The results presented here provide necessary data to model the excited state of C_3 using the method developed in Ref. [53].

[1] https://cdms.astro.uni-koeln.de.

5. Conclusions

High-resolution spectroscopy of the $\tilde{A}^1\Pi_u - \tilde{X}^1\Sigma_g^+$ transition of ^{13}C mono-substituted C_3 have been presented in this work. Rotationally resolved spectra of thirteen vibronic bands, eight of which belong to $^{13}C^{12}C^{12}C$ (000-000, 100-000, 02^+0-000, 02^-0-000, 04^+0-000, 04^-0-000, 12^-0-000, 002-000), and the other five belong to $^{12}C^{13}C^{12}C$ (000-000, 100-000, 02^+0-000, 02^-0-000, 04^-0-000), have been recorded and analysed. Except for the origin band of each isotopologue, the other bands are reported for the first time. The spectra carriers are confirmed by the rotational structures and the combination differences in the ground states, which are well known from previous studies [20,26]. The spectral linewidth is better than 0.023 cm^{-1}, corresponding to a resolution power of 10^6. The line positions are found to have an absolute frequency accuracy of 0.003 cm^{-1}. The spectroscopic constants for the upper vibronic states are determined from rotational analyses of the observed spectra. The results of the newly observed vibronic bands can be used to search for $^{13}C^{12}C^{12}C$ and $^{12}C^{13}C^{12}C$ in the optical region, with specific applications in diffuse and translucent interstellar clouds. The 100-000, 04^+0-000 and 12^-0-000 of $^{13}C^{12}C^{12}C$ and 02^+0-000 and 04^-0-000 of $^{12}C^{13}C^{12}C$ are best suited for this purpose since they are less blended by $^{12}C_3$ transitions.

Declaration of Competing Interest

The authors declare that they have no known competing financial interests or personal relationships that could have appeared to influence the work reported in this paper.

Acknowledgments

This work is supported by National Natural Science Foundation of China (21773221 and 21827804), the National Key R&D Program of China (2017YFA0303502), and the Fundamental Research Funds for the Central Universities of China (WK2340000078). HL acknowledges NWO, the Netherlands Organisation for Scientific Research, for financial support within the framework of a VICI grant.

Appendix A. Supplementary material

Supplementary data associated with this article can be found, in the online version, at https://doi.org/10.1016/j.jms.2021.111455.

References

[1] V. Wakelam, J.-C. Loison, E. Herbst, B. Pavone, A. Bergeat, K. Béroff, M. Chabot, A. Faure, D. Galli, W.D. Geppert, D. Gerlich, P. Gratier, N. Harada, K.M. Hickson, P. Honvault, S.J. Klippenstein, S.D. Le Picard, G. Nyman, M. Ruaud, S. Schlemmer, I.R. Sims, D. Talbi, J. Tennyson, R. Wester, The 2014 KIDA network for interstellar chemistry, Astrophys. J. Suppl. Series 217 (2015) 20, https://doi.org/10.1088/0067-0049/217/2/20.
[2] W. Huggins, Preliminary note on the photographic spectrum of comet b 1881, Proc. Roy. Soc. London 33 (216–219) (1882) 1–3, https://doi.org/10.1098/rspl.1881.0060.
[3] L. Gausset, G. Herzberg, A. Lagerqvist, B. Rosen, Analysis of the 4050Å Group of the C_3 Molecule, Astrophys. J. 142 (1965) 45, https://doi.org/10.1086/148262.
[4] A. McKellar, The far violet region in the spectra of the cool carbon stars, Astrophys. J. 108 (1948) 453, https://doi.org/10.1086/145080.
[5] U.G. Jørgensen, Dominating molecules in the photospheres of cool stars, in: U. G. Jørgensen (Ed.), Molecules in the Stellar Environment, Lecture Notes in Physics, Springer, Berlin, Heidelberg, 1994, pp. 29–48, https://doi.org/10.1007/3-540-57747-5-33.
[6] J.P. Maier, N.M. Lakin, G.A.H. Walker, D.A. Bohlender, Detection of C_3 in diffuse interstellar clouds, Astrophys. J. 553 (1) (2001) 267–273, https://doi.org/10.1086/320668.
[7] T. Oka, J.A. Thorburn, B.J. McCall, S.D. Friedman, L.M. Hobbs, P. Sonnentrucker, D.E. Welty, D.G. York, Observations of C_3 in translucent sight lines, Astrophys. J. 582 (2) (2003) 823–829, https://doi.org/10.1086/344726.

[8] G. Galazutdinov, A. Petlewski, F. Musaev, C. Moutou, G.L. Curto, J. Krełowski, The interstellar chain molecule in different interstellar environments, Astron. Astrophys. 395 (3) (2002) 969–974, https://doi.org/10.1051/0004-6361:20021324.

[9] E. Roueff, P. Felenbok, J.H. Black, C. Gry, Interstellar C_3 toward HD 210121, Astron. Astrophys. 384 (2) (2002) 629–637, https://doi.org/10.1051/0004-6361:20020067.

[10] M. Ádámkovics, G.A. Blake, B.J. McCall, Observations of rotationally resolved C_3 in translucent sight lines, Astrophys. J. 595 (1) (2003) 235, https://doi.org/10.1086/377305.

[11] M.R. Schmidt, J. Krełowski, G.A. Galazutdinov, D. Zhao, M.A. Haddad, W. Ubachs, H. Linnartz, Detection of vibronic bands of C_3 in a translucent cloud towards HD 169454, Mon. Not. R. Astron. Soc. 441 (2) (2014) 1134–1146, https://doi.org/10.1093/mnras/stu641.

[12] K.W. Hinkle, J.J. Keady, P.F. Bernath, Detection of C_3 in the circumstellar shell of IRC+10216, Science 241 (4871) (1988) 1319–1322, https://doi.org/10.1126/science.241.4871.1319.

[13] J. Cernicharo, J.R. Goicoechea, E. Caux, Far-infrared detection of C_3 in sagittarius B2 and IRC +10216*, Astrophys. J. Lett. 534 (2) (2000) L199, https://doi.org/10.1086/312668.

[14] T.F. Giesen, A.O.V. Orden, J.D. Cruzan, R.A. Provencal, R.J. Saykally, R. Gendriesch, F. Lewen, G. Winnewisser, Interstellar detection of CCC and high-precision laboratory measurements near 2 THz, Astrophys. J. Lett. 551 (2) (2001) L181, https://doi.org/10.1086/320024.

[15] B. Mookerjea, T. Giesen, J. Stutzki, J. Cernicharo, J.R. Goicoechea, M. De Luca, T. A. Bell, H. Gupta, M. Gerin, C.M. Persson, P. Sonnentrucker, Z. Makai, J. Black, F. Boulanger, A. Coutens, E. Dartois, P. Encrenaz, E. Falgarone, T. Geballe, B. Godard, P.F. Goldsmith, C. Gry, P. Hennebelle, E. Herbst, P. Hily-Blant, C. Joblin, M. Kaźmierczak, R. Kołos, J. Krełowski, D.C. Lis, J. Martin-Pintado, K.M. Menten, R. Monje, J.C. Pearson, M. Perault, T.G. Phillips, R. Plume, M. Salez, S. Schlemmer, M. Schmidt, D. Teyssier, C. Vastel, S. Yu, P. Dieleman, R. Güsten, C.E. Honingh, P. Morris, P. Roelfsema, R. Schieder, A.G.G.M. Tielens, J. Zmuidzinas, Excitation and abundance of C_3 in star forming cores: Herschel/HIFI observations of the sight-lines to W31C and W49N, Astron. Astrophys. 521 (2010) L13, https://doi.org/10.1051/0004-6361/201015095.

[16] B. Mookerjea, G.E. Hassel, M. Gerin, T. Giesen, J. Stutzki, E. Herbst, J.H. Black, P. F. Goldsmith, K.M. Menten, J. Krełowski, M. De Luca, T. Csengeri, C. Joblin, M. Kaźmierczak, M. Schmidt, J.R. Goicoechea, J. Cernicharo, Chemistry of C_3 and carbon chain molecules in DR21(OH), Astron. Astrophys. 546 (2012) A75, https://doi.org/10.1051/0004-6361/201219287.

[17] T.F. Giesen, B. Mookerjea, G.W. Fuchs, A.A. Breier, D. Witsch, R. Simon, J. Stutzki, First detection of the carbon chain molecules ^{13}CCC and C^{13}CC towards SgrB2(M), Astron. Astrophys. 633 (2020) A120, https://doi.org/10.1051/0004-6361/201936538.

[18] J. Baker, S.K. Bramble, P.A. Hamilton, A hot band LIF study of the $A^1\Pi_u - X^1\Sigma_g^+$ transition in C_3, Chem. Phys. Lett. 213 (3) (1993) 297–302, https://doi.org/10.1016/0009-2614(93)85135-B.

[19] W.J. Balfour, J. Cao, C.V.V. Prasad, C.X.W. Qian, Laser-induced fluorescence spectroscopy of the $A^1\Pi_u - X^1\Sigma_g^+$ transition in jet-cooled C3, J. Chem. Phys. 101 (12) (1994) 10343–10349, https://doi.org/10.1063/1.467914.

[20] A.A. Breier, T. Büchling, R. Schnierer, V. Lutter, G.W. Fuchs, K.M.T. Yamada, B. Mookerjea, J. Stutzki, T.F. Giesen, Lowest bending mode of ^{13}C-substituted C_3 and an experimentally derived structure, J. Chem. Phys. 145 (23) (2016) 234302, https://doi.org/10.1063/1.4971854.

[21] A.E. Douglas, Laboratory Studies of the lambda 4050 Group of Cometary Spectra, Astrophys. J. 114 (1951) 466, https://doi.org/10.1086/145486.

[22] R. Gendriesch, K. Pehl, T. Giesen, G. Winnewisser, F. Lewen I., Terahertz Spectroscopy of Linear Triatomic CCC: High Precision Laboratory Measurement and Analysis of the Ro-Vibrational Bending Transitions, Zeitschrift für Naturforschung A 58 (2–3) (2003). doi:10.1515/zna-2003-2-310.

[23] M. Haddad, D. Zhao, H. Linnartz, W. Ubachs, Rotationally resolved spectra of the 4051Å comet band of C_3 for all six ^{12}C and ^{13}C isotopologues, J. Mol. Spectrosc. 297 (2014) 41–50, https://doi.org/10.1016/j.jms.2014.01.010.

[24] M. Izuha, K. Yamanouchi, New A-X vibronic bands of laser-vaporized C_3, J. Chem. Phys. 109 (5) (1998) 1810–1818, https://doi.org/10.1063/1.476756.

[25] K. Kawaguchi, K. Matsumura, H. Kanamori, E. Hirota, Diode laser spectroscopy of C3: The $\nu_2 + \nu_3 - \nu_2, 2\nu_2 + \nu3 - 2\nu_2$, and $2\nu_2 + \nu_3$ bands, J. Chem. Phys. 91 (4) (1989) 1953–1957, https://doi.org/10.1063/1.457054.

[26] J. Krieg, V. Lutter, C.P. Endres, I.H. Keppeler, P. Jensen, M.E. Harding, J. Vázquez, S. Schlemmer, T.F. Giesen, S. Thorwirth, High-resolution spectroscopy of C_3 around 3 μm, J. Phys. Chem. A 117 (16) (2013) 3332–3339, https://doi.org/10.1021/jp3119204.

[27] K. Matsumura, H. Kanamori, K. Kawaguchi, E. Hirota, Infrared diode laser kinetic spectroscopy of the $\nu3$ band of C_3, J. Chem. Phys. 89 (6) (1988) 3491–3494, https://doi.org/10.1063/1.454919.

[28] B. McCall, R. Casaes, M. Ádámkovics, R. Saykally, A re-examination of the 4051 Å band of C_3 using cavity ringdown spectroscopy of a supersonic plasma, Chem. Phys. Lett. 374 (5–6) (2003) 583–586, https://doi.org/10.1016/S0009-2614(03)00769-3.

[29] N. Moazzen-Ahmadi, A.R.W. McKellar, Infrared diode laser spectroscopy of the $\nu3$ fundamental and $\nu_3 + \nu_2 - \nu_2$ sequence bands of ^{13}C3 and of the ν_3 fundamental band of ^{12}C ^{12}C^{12}C, J. Chem. Phys. 98 (10) (1993) 7757–7762, https://doi.org/10.1063/1.464583.

[30] F. Northrup, T.J. Sears, Observation of stimulated emission pumping spectra of jet-cooled NCS and C_3, Chem. Phys. Lett. 159 (5–6) (1989) 421–425, https://doi.org/10.1016/0009-2614(89)87510-4.

[31] F.J. Northrup, T.J. Sears, Stimulated-emission pumping spectroscopy study of jet-cooled C_3: Pure bending levels and bend–symmetric-stretch combination levels of $X^1\Sigma_g^+$, JOSA B 7 (9) (1990) 1924–1934, https://doi.org/10.1364/JOSAB.7.001924.

[32] C.M.R. Rocha, A.J.C. Varandas, Accurate ab initio -based double many-body expansion potential energy surface for the adiabatic ground-state of the C_3 radical including combined Jahn-Teller plus pseudo-Jahn-Teller interactions, J. Chem. Phys. 143 (7) (2015) 074302, https://doi.org/10.1063/1.4928434.

[33] E.A. Rohlfing, Laser-induced-fluorescence spectroscopy of jet-cooled C_3, J. Chem. Phys. 91 (8) (1989) 4531–4542, https://doi.org/10.1063/1.456791.

[34] E.A. Rohlfing, J.E.M. Goldsmith, Stimulated-emission pumping spectroscopy of jet-cooled C_3: Antisymmetric stretch–bend levels, J. Opt. Soc. Am. B 7 (9) (1990) 1915, https://doi.org/10.1364/JOSAB.7.001915.

[35] C.A. Schmuttenmaer, R.C. Cohen, N. Pugliano, Heath, A.L. Cooksy, K.L. Busarow, R.J. Saykally, Tunable far-IR laser spectroscopy of jet-cooled carbon clusters: The νC_2 bending vibration of C_3, Science 249 (4971) (1990) 897–900, https://doi.org/10.1126/science.11538082.

[36] B. Schröder, K.D. Doney, P. Sebald, D. Zhao, H. Linnartz, Stretching our understanding of C_3: Experimental and theoretical spectroscopy of highly excited $n\nu_1 + m\nu_3$ states ($n \leq 7$ and $m \leq 3$), J. Chem. Phys. 149 (1) (2018) 014302, https://doi.org/10.1063/1.5034092.

[37] A. Tanabashi, T. Hirao, T. Amano, P.F. Bernath, Fourier transform emission spectra of the (000)-(000) Band of the Λ4051.6 Band of C_3, Astrophys. J. 624 (2) (2005) 1116, https://doi.org/10.1086/429316.

[38] D.W. Tokaryk, D.E. Chomiak, Laser spectroscopy of C_3: Stimulated emission and absorption spectra of the $A^1\Pi_u - X^1\Sigma_g^+$ transition, J. Chem. Phys. 106 (18) (1997) 7600–7608, https://doi.org/10.1063/1.473762.

[39] G. Zhang, K.-S. Chen, A.J. Merer, Y.-C. Hsu, W.-J. Chen, S. Shaji, Y.-A. Liao, The 4051-Å band of C_3 ($A^1\Pi_u - X^1\Sigma_g^+$, 000–000): Perturbed low-J lines and lifetime measurements, J. Chem. Phys. 122 (24) (2005) 244308, https://doi.org/10.1063/1.1928827.

[40] K. Clusius, A.E. Douglas, THE Λ4050 bands of the C_3^{13} molecule, Can. J. Phys. 32 (5) (1954) 319–325, https://doi.org/10.1139/p54-030.

[41] B. Schröder, P. Sebald, High-level theoretical rovibrational spectroscopy beyond fc-CCSD(T): The C_3 molecule, J. Chem. Phys. 144 (4) (2016) 044307, https://doi.org/10.1063/1.4940780.

[42] W.D. Langer, T.E. Graedel, M.A. Frerking, P.B. Armentrout, Carbon and oxygen isotope fractionation in dense interstellar clouds, Astrophys. J. 277 (1984) 581–590, https://doi.org/10.1086/161730.

[43] Q. Zhang, D.-P. Zhang, B.-X. Zhu, J.-W. Gu, D.-F. Zhao, Y. Chena, Reinvestigate the $C2_\Pi - X_2\Pi$ (0,0) band of AgO, Chin. J. Chem. Phys. 33 (1) (2020) 75–78, https://doi.org/10.1063/1674-0068/cjcp1912223.

[44] Q. Zhang, D. Zhang, B. Zhu, J. Gu, Z. Xiao, C. Yu, Y. Chen, D. Zhao, Rotationally resolved spectrum of the $B^1A' - X^1A'$ 0 0 0 band of CuSH, J. Mol. Spectrosc. 350 (2018) 27–29, https://doi.org/10.1016/j.jms.2018.05.007.

[45] B. Zhu, J. Gu, C. Yu, Z. Xiao, Y. Chen, D. Zhao, High-resolution laser spectroscopic survey of the $H^3\Sigma_u$—$X^3\Sigma_g$-Electronic Transition of Si2, J. Phys. Chem. A 124 (15) (2020) 2972–2981, https://doi.org/10.1021/acs.jpca.0c00370.

[46] D. Zhang, Q. Zhang, B. Zhu, J. Gu, B. Suo, Y. Chen, D. Zhao, High-resolution electronic spectra of yttrium oxide (YO): The $D^2\Sigma^+ - X^2\Sigma^+$ transition, J. Chem. Phys. 146 (11) (2017) 114303, https://doi.org/10.1063/1.4978335.

[47] Q. Zhang, B. Zhu, D. Zhang, J. Gu, D. Zhao, Y. Chen, Note: Pulsed single longitudinal mode optical parametric oscillator for sub-Doppler spectroscopy of jet cooled transient species, Rev. Sci. Instrum. 88 (12) (2017) 126108, https://doi.org/10.1063/1.5009962.

[48] C.M. Western, PGOPHER: A program for simulating rotational, vibrational and electronic spectra, J. Quant. Spectrosc. Radiat. Transfer 186 (2017) 221–242, https://doi.org/10.1016/j.jqsrt.2016.04.010.

[49] B.A. McGuire, 2018 Census of interstellar, circumstellar, extragalactic, protoplanetary disk, and exoplanetary molecules, Astrophys. J. Suppl. Series 239 (2) (2018) 17, https://doi.org/10.3847/1538-4365/aae5d2.

[50] N. Sakai, S. Takano, T. Sakai, S. Shiba, Y. Sumiyoshi, Y. Endo, S. Yamamoto, Anomalous 13C Isotope Abundances in C3S and C4H Observed toward the Cold Interstellar Cloud, Taurus Molecular Cloud-1, J. Phys. Chem. A 117 (39) (2013) 9831–9839, https://doi.org/10.1021/jp3127913.

[51] S. Takano, A. Masuda, Y. Hirahara, H. Suzuki, M. Ohishi, S.-I. Ishikawa, N. Kaifu, Y. Kasai, K. Kawaguchi, T.L. Wilson, Observations of 13)C isotopomers of HC_(3)N and HC_(5)N in TMC-1: Evidence for isotopic fractionation, Astron. Astrophys. 329 (1998) 1156–1169. http://adsabs.harvard.edu/abs/1998A%26A...329.1156T.

[52] K. Furuya, Y. Aikawa, N. Sakai, S. Yamamoto, Carbon isotope and isotopomer fractionation in cold dense cloud cores, Astrophys. J. 731 (1) (2011) 38, https://doi.org/10.1088/0004-637X/731/1/38.

[53] A.A. Breier, T.F. Giesen, S.C. Ross, K.M.T. Yamada, Improved bond length determination technique for C_3 and other linear molecules with a large amplitude bending vibration, J. Mol. Struct. 1219 (2020) 128329, https://doi.org/10.1016/j.molstruc.2020.128329.